https://doi.org/10.5194/amt-2024-99
Preprint. Discussion started: 11 June 2024

Atmospheric Measurement Techniques Discussions

JAXA Level 2 cloud and precipitation microphysics retrievals based on EarthCARE CPR, ATLID and MSI

Kaori Sato[1], Hajime Okamoto[1], Tomoaki Nishizawa[2], Yoshitaka Jin[2], Takashi Y. Nakajima[3], Minrui Wang[3], Masaki Satoh[4], Woosub Roh[4,5], Hiroshi Ishimoto[6], Rei Kudo[6]

[1] Research Institute for Applied Mechanics, Kyushu University, Fukuoka, 816-8580, Japan
[2.]Earth System Division, National Institute for Environmental Studies, Tsukuba, 305-8506, Japan
[3.]Research & Information Center, Tokai University, Kanagawa, 2591292, Japan
[4.]Atmosphere and Ocean Research Institute, The University of Tokyo, Chiba, 2778564, Japan
[5.]Tokyo University of Marine Science and Technology, Tokyo, 1358533, Japan
[6] Meteorological Research Institute, Japan Meteorological Agency, Tsukuba, 305-0052, Japan

Correspondence to: Kaori Sato (sato@riam.kyushu-u.ac.jp)

Abstract

This study introduces the primary products and features of active sensor-based Level 2 cloud products of the Japanese Aerospace Exploration Agency (JAXA). Combined with 94 GHz Doppler cloud radar and 355-nm high-spectral-resolution lidar, these products provide a detailed view of the transitions of cloud particle categories and their size distributions, as well as vertical velocity information. Simulated EarthCARE Level 1 data mimicking actual global observations were used to assess the performance of the JAXA Level 2 cloud product. Evaluation of the product revealed that the retrievals reasonably reproduced the vertical profile of the modelled microphysics. Further validation of the products is planned for after-launch calibration/validation. JAXA Level 2 velocity-related products will be described in a future paper.

1. Introduction

With advances in high-resolution global cloud-resolving models for climate simulations, there is increasing interest in the observation of global vertical velocity and cloud property information. Vertical velocity distributions are important for hydrometeor formation (Sullivan et al., 2016) and EarthCARE will provide the first dense global observations. A method for the simultaneous retrieval of air motion, particle sedimentation velocity, and microphysics using similar variables obtainable by EarthCARE cloud profiling radar (CPR) and atmospheric lidar (ATLID) has been developed and tested using the Equatorial Atmospheric Radar (Sato et al., 2009). Information derived using this method was used to investigate ice water content in relation to convective activity to evaluate an atmospheric general circulation model (Sato et al., 2010). It is anticipated that analyses of EarthCARE data will be useful for quantifying the role of vertical velocity in determining cloud properties and lifetime. The lidar depolarization measurement is a strong indicator of particle phase, shape, and orientation (Yoshida et al., 2010). Radar-lidar synergy algorithm with a specular reflection mode investigated the mass mixing ratio of oriented plates (2D types) and randomly oriented crystals (3D ice) within clouds (Okamoto et al., 2010) and ice precipitation

https://doi.org/10.5194/amt-2024-99
Preprint. Discussion started: 11 June 2024


Atmospheric Measurement Techniques Discussions

(Sato and Okamoto, 2011) at each vertical grids from CloudSat and Cloud Aerosol Lidar and Infrared Pathfinder Satellite Observations (CALIPSO) data. The recent development of numerical simulations of lidar backscattering for interpreting 355-nm high-spectral resolution polarization lidar (HSRL) measurements has demonstrated the possibility of deriving more specific ice habit category information from EarthCARE, in addition to the cloud phase and 2D/3D ice category. Measurements from ground-based HSRL support such theoretical studies (Jin et al., 2020, 2022). These unique aspects are incorporated into active sensor-based Japanese Aerospace Exploration Agency (JAXA) Level 2 (L2) cloud algorithms to create products that beneficial for investigating cloud formation and cloud-precipitation processes. A preliminary study of the JAXA L2 cloud product using available satellite data produced exciting results, displaying a unique geographical preference for the occurrence and height-dependent characteristics of different ice habit categories (Sato and Okamoto, 2023). Each component of the EarthCARE L2 products should significantly increase our understanding of the coupling of cloud microphysics, radiation, and dynamics.

This paper is organized as follows. Section 2 provides an overview of active sensor-based JAXA L2 cloud products and simulated EarthCARE Level 1 (L1) data. The JAXA L2 cloud product is demonstrated and assessed in Section 3. Section 4 summarizes the results and outlines future expectations for EarthCARE that has been successfully launched into orbit on 28 May (15:20 local time).

2. Data and description

2.1 Overview of JAXA Level 2 Cloud Product

The JAXA L2 active sensor-based cloud product has three different algorithm-processing chains: the standalone product (CPR_CLP), the CPR–ATLID synergy cloud product (AC_CLP), and the CPR–ATLID–Multispectral Instrument (MSI) product (ACM_CLP). Table 1 summarizes the primary cloud products from each algorithm package. Standard (ST) JAXA L2 cloud products will be released earlier, and the JAXA L2 research cloud products will be released later and will be processed in the JAXA Earth Observation Research Center Research and Application System (ER) or JAXA Laboratories (LR). JAXA L2 research cloud products include velocity-related products such as sedimentation velocity and air motion (Sato et al., 2009) and microphysics obtained using L2 CPR Doppler velocity; details of these research products will be reported in a future paper. All products are reported using the Joint Standard Grid (JSG) with 1 km horizontal and 100 m vertical grid spacing. Details of the cloud mask and cloud particle type products (i.e., cloud phase and ice particle orientation) are reviewed in Okamoto et al. (2024).

https://doi.org/10.5194/amt-2024-99
Preprint. Discussion started: 11 June 2024

Atmospheric Measurement Techniques Discussions

Product	Discription	CPR_CLP (L2a CPR)	AC_CLP (L2b CPR-ATLID)	ACM_CLP (L2b CPR-ATLID-MSI)
cloud mask	cloud+precipitation (Described in Okamoto et al., AMT, 2024) clear/warm water/ supercooled water /3d ice /2d plate /mixture of 3d ice and 2d plate / liquid drizzle / mixed-phase drizzle / rain / snow / water+liquid drizzle / water+rain / mixed-phase / melting layer	✔ST	✔ST	✔ST
cloud particle type		✔ST	✔ST	✔ST
ice particle category	dominant ice particle habit categories (2Dplate, 2Dcolumn, bullet rosette/3Daggregates, droxtal, voronoi, fractal)	✔ST	✔ST	✔ST
cloud water effective radius	cloud+precipitation, Both liquid-phase and ice-phase microphysics are reported at each vertical grid	✔ST	✔ST	✔ST
cloud ice effective radius		✔ST	✔ST	✔ST
cloud water content		✔ST	✔ST	✔ST
cloud ice content		✔ST	✔ST	✔ST
total cloud water number concentration		✔ST	✔ST	✔ST
total cloud ice number concentration		✔ST	✔ST	✔ST
- cloud effective radius1 (1)	Subcategory products to infer particle size distribution of cloud and precipitation Cloud phase 1 and 2 : (0) not retrieved, (1) water, (2) ice, (-9) clear combination of ice+ice, water+water, ice+water are possible Effective radius and water content corresponding to cloud phase 1 and 2 are reported at each vertical grid	✔ST	✔ST	✔ST
- cloud effective radius2 (2)		✔ST	✔ST	✔ST
- cloud water content1		✔ST	✔ST	✔ST
- cloud water content2		✔ST	✔ST	✔ST
- cloud phase1		✔ST	✔ST	✔ST
- cloud phase2		✔ST	✔ST	✔ST
optical thickness	Liquid + Ice phase	✔ST	✔ST	✔ST
cloud water path		✔ST	✔ST	✔ST
cloud ice water path		✔ST	✔ST	✔ST
Rain Rate	vertical profile	✔ER/LR	✔ER/LR	✔ER/LR
Snow Rate	vertical profile	✔ER/LR	✔ER/LR	✔ER/LR
cloud doppler velocity	In-cloud Doppler velocity with folding correction reported after applying cloud mask	✔ER/LR	✔ER/LR	✔ER/LR
total cloud terminal velocity	Mean terminal velocity pf cloud and precipitation particles	✔ER/LR	✔ER/LR	✔ER/LR
- cloud terminal velocity1	Terminal velocity corresponding to (1) and (2)	✔ER/LR	✔ER/LR	✔ER/LR
- cloud terminal velocity2		✔ER/LR	✔ER/LR	✔ER/LR
cloud air velocity	In-cloud vertical air velocity	✔ER/LR	✔ER/LR	✔ER/LR

Table 1: Primary parameters of the Japanese Aerospace Exploration Agency (JAXA) Level 2 (L2) standard (ST) and research (ER/LR) active sensor-based cloud products, including the standalone product (CPR_CLP), the CPR–ATLID synergy cloud product (AC_CLP), and the CPR–ATLID–MSI product (ACM_CLP). The ER and LR products will be processed in the JAXA Earth Observation Research Center Research and Application System and JAXA Laboratories, respectively. ATLID, atmospheric lidar CPR, cloud profiling radar; MSI, Multispectral Instrument.

https://doi.org/10.5194/amt-2024-99
Preprint. Discussion started: 11 June 2024

Atmospheric Measurement Techniques Discussions

2.2 Processing flow of the JAXA Level 2 cloud product

Figure 1 shows the flow of the L2 cloud products. CPR_CLP and ACM_CLP share the same basic algorithm with AC_CLP, and in CPR_CLP, the ATLID observables are simulated based on observations to drive the AC_CLP-like retrieval, and ACM_CLP has additional treatments to handle inputs from MSI. The JAXA L2 Echo product processes CPR L1 data and was developed by the National Institute of Information and Communications Technology (NICT). The major inputs from the JAXA L2 Echo product to CPR_CLP, AC_CLP, and ACM_CLP are radar reflectivity (Z_e), Doppler velocity (V_D), normalized radar cross-section (σ_0)/pulse integrated attenuation (PIA), gaseous attenuation, clutter mask, and quality flags. The inputs from the JAXA L2 ATLID product (Nishizawa et al., 2024) to the AC_CLP and ACM_CLP algorithms are L2 ATLID observables (i.e., extinction coefficient α_{ext}, backscattering coefficient β, and depolarization ratio δ) and their aerosol and cloud components (Kudo et al., 2016; Kudo et al., 2023), the ALTID-only cloud mask, cloud type (Okamoto et al., 2024), ice particle category (Sato and Okamoto, 2023). The aerosol extinction is used to consider attenuation due to aerosols above the cloud layers. The inputs from the JAXA L2 MSI products to ACM_CLP are the optical thickness and effective radius of the ice and liquid phases (Nakajima et al., 2019; Wang et al., 2023), which are used to constrain CPR_CLP and AC_CLP microphysics estimates. The JAXA Level 2 cloud product is further handled by the JAXA L2 four-sensor radiation products (Yamauchi et al., 2024).

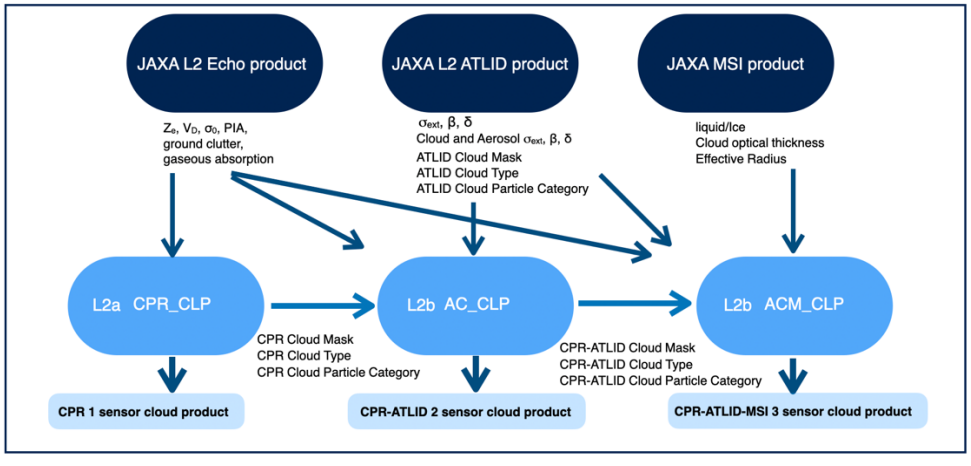

Figure 1: Flow of the Japanese Aerospace Exploration Agency (JAXA) Level 2 (L2) cloud products, including the standalone product (CPR_CLP), the CPR–ATLID synergy cloud product (AC_CLP), and the CPR–ATLID–MSI product (ACM_CLP). ATLID, atmospheric lidar CPR, cloud profiling radar; MSI, Multispectral Instrument.

https://doi.org/10.5194/amt-2024-99
Preprint. Discussion started: 11 June 2024


Atmospheric Measurement Techniques Discussions

2.3 Description of the JAXA Level 2 cloud product

The following briefly describes the highlights of the standard JAXA L2 cloud products. The details of each method are provided in the JAXA Algorithm Theoretical Basis Document (ATBD). After applying cloud mask and cloud phase discrimination schemes (Okamoto et al., 2024), one of the main products of the JAXA L2 cloud product is the ice particle category product, which enables a more detailed comprehensive exploration of the dominant ice particle habit category contained within each JSG grid. The ice particle categories are identified based on ATLID lidar ratio and depolarization ratio diagrams (Okamoto et al., 2019; 2020; Sato and Okamoto, 2023). This information is anticipated to be instrumental for remote sensing applications (Van Diedenhoven, 2018; Letu et al., 2016) and the development of ice optical parameterization (Li et al. 2022) and sedimentation velocity parameterization for use in numerical models. The retrieved ice particle habit categories are horizontally oriented two-dimensional (2D) plates and their assemblages, 2D columns and their assemblages, bullet rosettes and three-dimensionally (3D) oriented aggregate types, droxtal/compact types, voronoi/irregular/roughened types, and fractal type snow aggregates (Ishimoto et al., 2008, 2012). The ATLID-based ice particle category product is developed and reported from the JAXA L2 cloud algorithms but will also be reported from the JAXA L2 ATLID product (ATL-CLA; Nishizawa et al., 2024). This ATLID-based classification method is trained to be produced from CPR observables for cloud scenes where the ATLID signals are limited, and is produced using the CPR_CLP, AC_CLP, and ACM_CLP algorithms. An algorithm to retrieve the microphysical properties of mixture of two particle types (i.e., 2D and 3D ice) has been developed for ice cloud regions observed with CloudSat and CALIPSO synergy (Okamoto et al., 2010). A framework to extend the applicability of the microphysics retrieval algorithm from the cloud region to the entire precipitating region in the vertical column was developed by efficiently reflecting the information from the lidar-radar overlap region to the microphysical retrieval at the CloudSat or CALIPSO-only region (Sato et al., 2011, 2020). The L2 cloud microphysics retrieval algorithms further extend previous algorithms and use forward models for each sensor corresponding to the derived ice particle categories, i.e., microphysics corresponding to each category can be obtained. The single scattering properties of ice particles with various shapes and orientations are calculated using physical optics (Borovoi et al., 2012) and modified geometrical optics integral equation methods (Masuda et al., 2012) for the ATLID specification and using the discrete dipole approximation and finite time domain method for the CPR wavelength, and multiple scattering effects are estimated based on Sato et al. (2018, 2019). ATLID σ_{ext}, δ, and β are used to derive the effective radius and water content of liquid and ice clouds, and the synergy among ATLID observables, CPR Z_e, and σ_0/PIA are used to further determine the microphysics for the entire cloud and precipitation regions (Sato et al., 2018, 2019; Sato and Okamoto, 2020). For each cloudy JSG grid, the particle type discrimination scheme (Kikuchi et al., 2017; Okamoto et al., 2024) identifies the mixed phase, transition from ice to snow particles, precipitation types, and their co-existence with liquid cloud particles. The cloud microphysics scheme considers the maximum of two different size distributions at each JSG grid to provide details of the particle size distribution (Table 1.).

https://doi.org/10.5194/amt-2024-99
Preprint. Discussion started: 11 June 2024

Atmospheric Measurement Techniques Discussions

2.4 JAXA joint simulator-derived EarthCARE L1 data

The performance of the JAXA L2 cloud algorithms was tested using simulated EarthCARE L1 orbit data created by the JAXA joint simulator (Roh et al., 2023 and references therein). These L1 data are created using cloud and precipitation scenes generated by the Nonhydrostatic Icosahedral Atmospheric Model (NICAM) (Satoh et al., 2014) at 3.5-km horizontal resolution, and profiles of aerosol species simulated by the NICAM Spectral Radiation–Transport Model. Random errors and noise are added to create CPR and ATLID signals, and the spectral misalignment effect of the visible and near-infrared channels is introduced for the MSI (Roh et al., 2023) to mimic actual observations. The simulated L1 data for an EarthCARE orbit are divided into eight frames, and 15 frames are simulated to cover representative cloud and aerosol scenes over the globe. All 15 frames are used to evaluate the JAXA L2 cloud product.

3. Demonstration and assessment of JAXA Level 2 cloud product

Figure 2 shows the ice particle category product, which was derived using complementary observations from Cloud-Aerosol Lidar and Infrared Pathfinder Satellite Observations (CALIPSO) and Cloud-Aerosol Lidar with Orthogonal Polarization (CALIOP) (Sato and Okamoto, 2023). The CALIPSO data was combined onto the CloudSat grid with a resolution of 240 m vertically and 1 km horizontally (Kyushu University (KU) CloudSat-CALIPSO Merged Data set data; Hagihara et al., 2010). Lidar ratio and depolarization ratio information from ATLID may offer a more robust classification of ice particle categories and orientations, and long-term analysis from CALIOP to ATLID will increase the reliability of the product (Okamoto et a., 2020). The EarthCARE L2 data will be provided at 100 m vertical resolution.

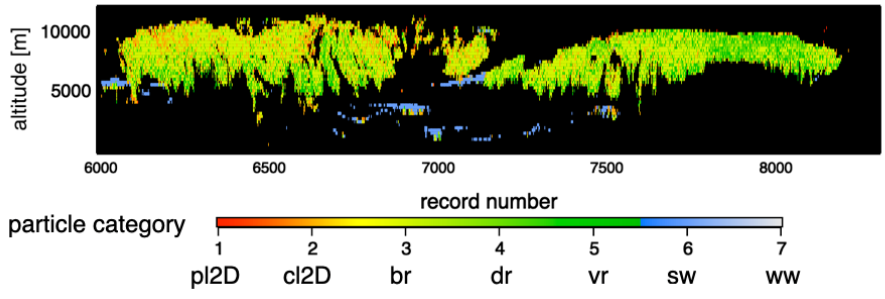

Figure 2: Demonstration of the JAXA L2 ice particle category product. The dominant ice category type is classified into [1]2D plate (pl2D), [2]2D column (cl2D), [3]3D bullet (bullet rosettes, 3D aggregate category) (br), [4] Droxtals (dr), and [5] Voronoi types (vr), [6] supercooled water (sw), [7] warm water (ww). The JAXA EarthCARE L2 cloud algorithms were modified to be applied to A-Train data, and the ice category classification was derived using Cloud-Aerosol Lidar with Orthogonal Polarization (CALIOP).

Cloud microphysics retrieved from the simulated EarthCARE L1 data are compared with the truth. For the comparison, we used the AC_CLP standard products. Figure 3 shows an example of the time–height cross-section of the simulated CPR

https://doi.org/10.5194/amt-2024-99
Preprint. Discussion started: 11 June 2024

Atmospheric Measurement Techniques Discussions

measurements and the ATLID L2 cloud backscatter for a cirrus case (scene 1), snow precipitation (scene 2), and a liquid-
150 phase cloud scene (scene 3). Overall, there was good consistency between the simulated and retrieved cloud water contents and effective radius, where the AC_CLP standard retrievals reasonably reproduced vertical variation in the microphysical properties seen in the model (Fig. 4-6).

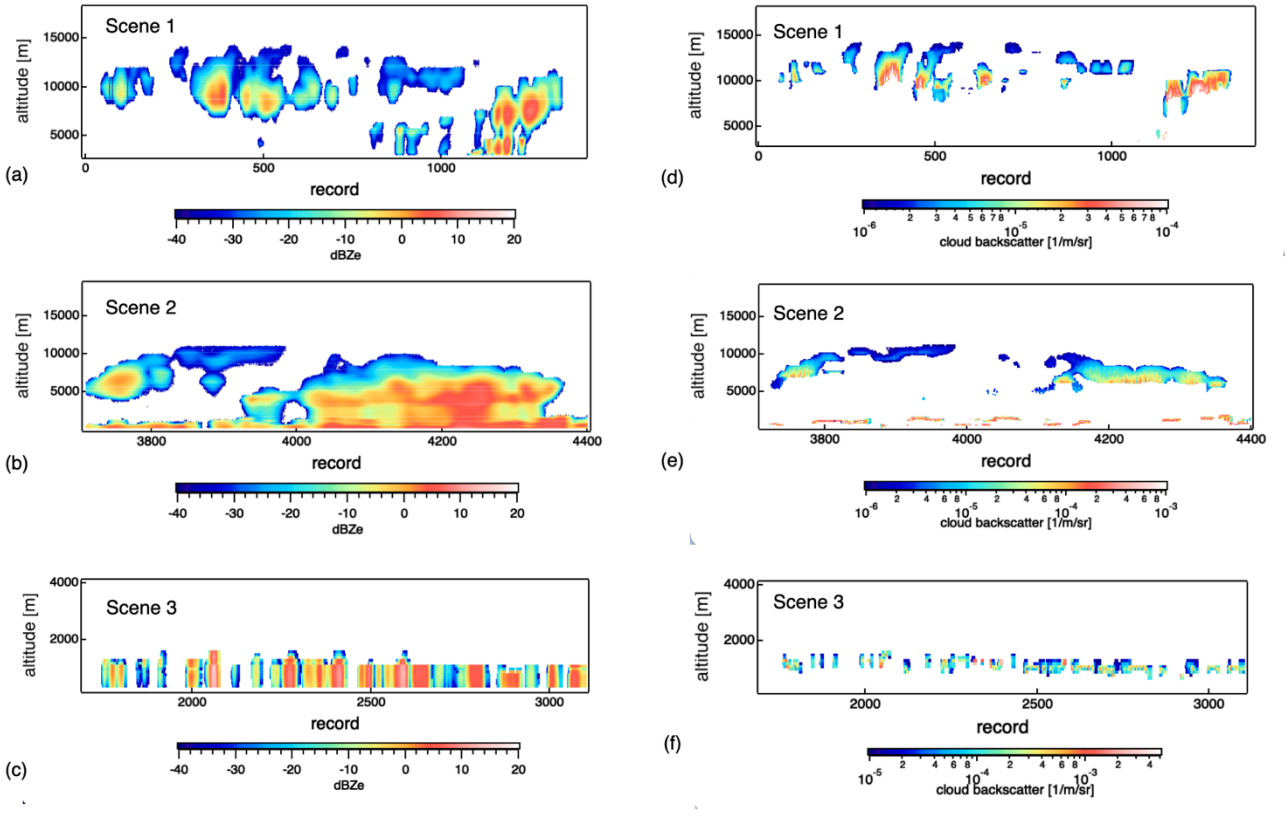

155

Figure 3: Inputs of CPR Ze measurements simulated using the JAXA joint simulator and ATLID L2 cloud backscatter product for different cloud scenes. (a)(d) Scene 1 is a cirrus case, (b)(e) scene 2 is a case with more ice precipitations, and (c)(f) scene 3 is dominated by liquid-phase.

https://doi.org/10.5194/amt-2024-99
Preprint. Discussion started: 11 June 2024

Atmospheric Measurement Techniques Discussions

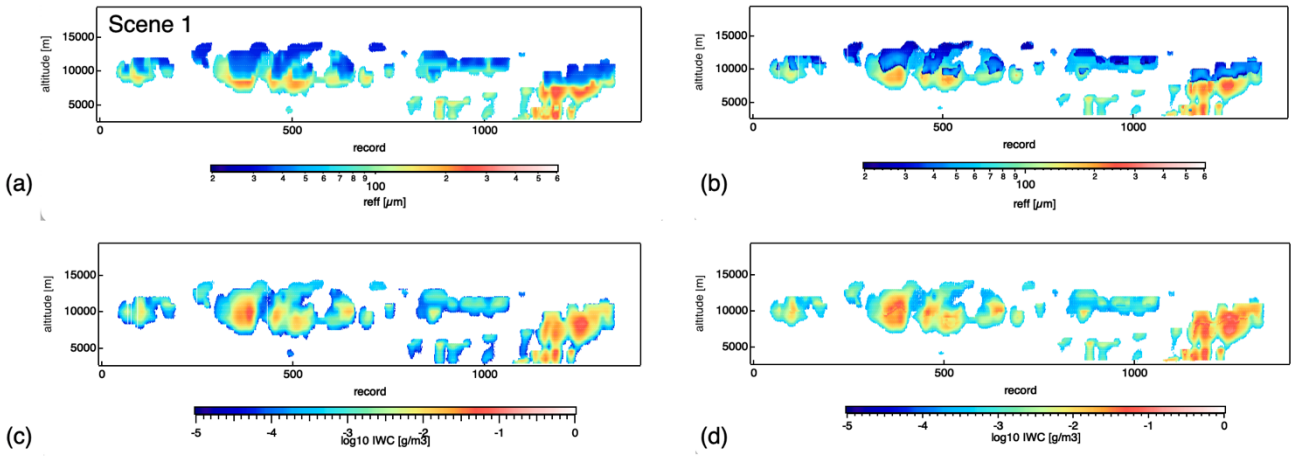

Figure 4: Time–height cross-section of (a, c) simulated and (b, d) retrieved effective radius and total water content for ice-phase corresponding to scene 1 in Fig.3(a).

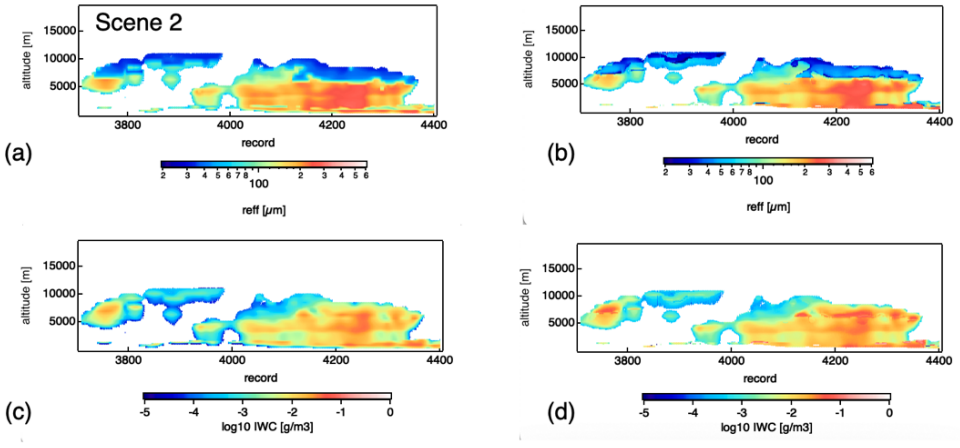

Figure 5: Time–height cross-section of (a, c) simulated and (b, d) retrieved effective radius and total water content for scene 2 in Fig.3 (b).

https://doi.org/10.5194/amt-2024-99
Preprint. Discussion started: 11 June 2024

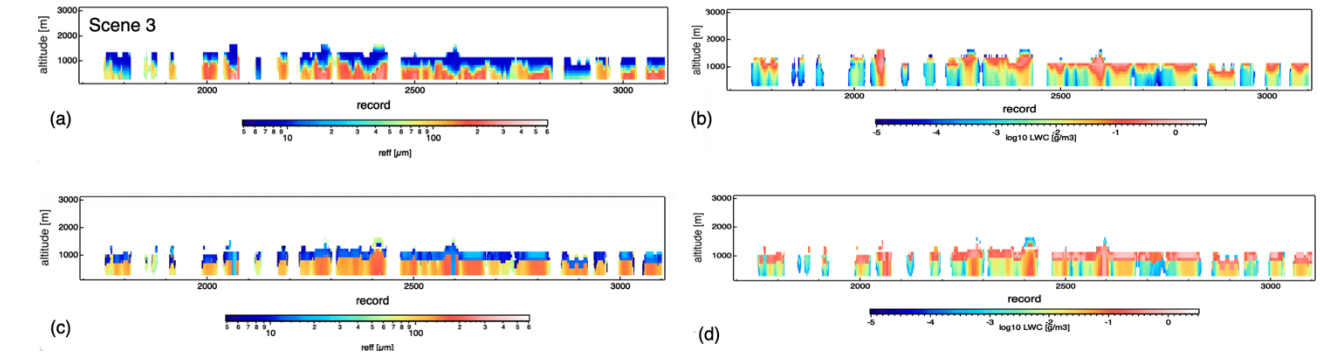

Figure 6: Time–height cross-section of (a, b) simulated and (c, d) retrieved effective radius and total water content for a liquid-phase case corresponding to scene 3 in Fig.3 (c).

175

We also performed a one-to-one comparison of retrieved (ret) and modeled (JS) effective radius ($r_{eff,ret}$ and $r_{eff,JS}$), ice water content (IWC_{ret} and IWC_{JS}), and liquid water content (WC_{ret} and WC_{JS}) at each JSG grid for AC_CLP using all 15 EarthCARE frames of the simulated observation data (Fig. 7, 8). The results showed that for both the ice and liquid phases, the majority of the retrieved population of r_{eff} and water content lay close to the 1:1 line. For the ice phase, the slopes of the
180 regression lines were generally around 0.8 and ice water content had about 14.5% mean relative error and tended to be slightly overestimated when the ice water content were small (Fig. 7a). The effective radius of ice phase was evaluated at small (Fig.7b) and large size ranges (Fig.7c) bounded at 60μm. In the model, three modes (i.e., ice cloud particles, snow, and graupel) contributes to the effective radius for the ice phase. Despite such complexity, the mean relative error of the effective radius retrievals for the larger size range was about 28.9%, and mean relative errors and the mean bias of the effective radius
185 retrievals for the smaller size range were about 18.6% and 7.5%, respectively.

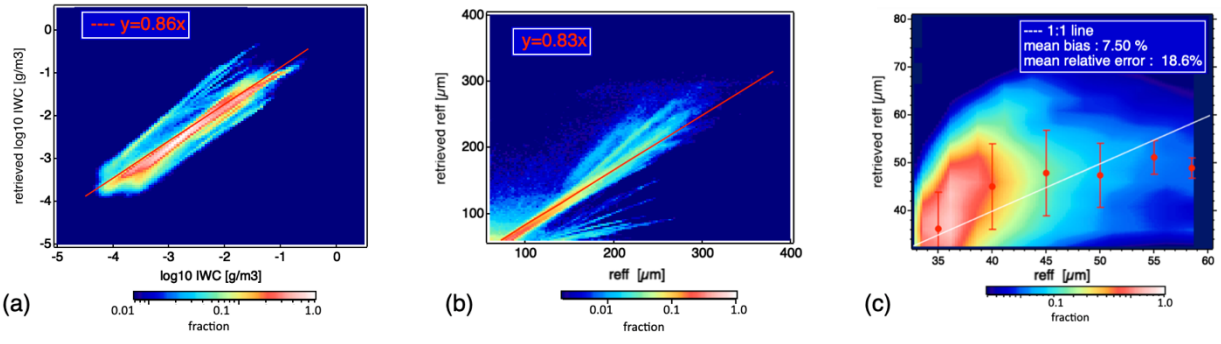

Figure 7: Scatterplot of retrieved and modelled (a) ice water content and (b)(c) ice phase effective radius. Red and white solid lines correspond to a linear regression line forced through the origin and a 1:1 ratio, respectively. Symbols in (c) indicate means and
190 **standard deviation of retrieved r_{eff}.**

https://doi.org/10.5194/amt-2024-99
Preprint. Discussion started: 11 June 2024

Atmospheric Measurement Techniques Discussions

The liquid water content retrievals for the water clouds were able to track the change in the liquid water content and corresponded relatively well with the model truth. A larger scatter around the truth was observed at larger liquid water content range, which was biased low. Further analysis of the model suggested that this could in part occurred when liquid cloud particles made a major contribution to the water content, but a negligible contribution to Z_e and its vertical structure, which in some cases the algorithm made a slight misinterpretation when determining their contributions at the CPR-only regions. The slopes of the regression lines were also around 0.8 for both liquid water content and effective radius of liquid precipitation (Fig.8a, b). For the smaller size range, the frequency distribution of the retrieved effective radius was examined since the liquid cloud particles in the model has a constant effective radius of 8 μm (Fig.8c). It was seen that the retrieved peak size was close to the model truth and was around 10 μm, which was about 2 μm overestimation, and smaller fraction of drizzle -sized particle was also retrieved. In future, we will further investigate the improvement in the microphysics retrieval when the ACM_CLP algorithm with CPR–ATLID–MSI synergy was applied to the simulated EarthCARE L1 data.

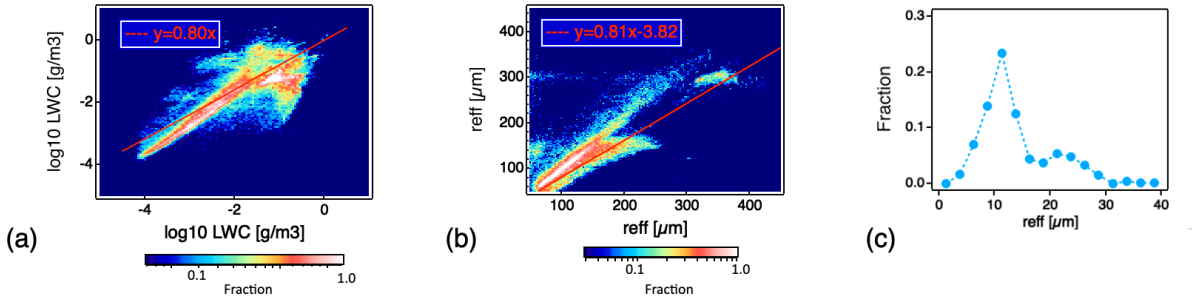

Figure 8: Scatterplot of retrieved and modelled (a) liquid water content and (b) effective radius of liquid precipitation. Frequency distribution of the retrieved effective radius of cloud particles is shown in (c). Solid lines correspond to a linear regression line.

4. Summary and Expectations

This study introduces the active sensor-based JAXA L2 cloud product, which is produced using three different algorithm-processing chains. The L2a CPR_CLP chain produces the standalone CPR cloud product; L2b AC_CLP produces the CPR–ATLID synergy cloud product; and L2b ACM_CLP produces the CPR–ATLID–MSI synergy cloud product. The cloud microphysics scheme considers the maximum of two different size distributions at each JSG grid to treat and capture the co-existence of cloud and precipitation particles or particles with different cloud phases. For the EarthCARE mission, the outputs from the JAXA L2 standard cloud product feature a 3D global view of the dominant ice habit categories and microphysics, and habit and size distribution transitions from cloud to precipitation. Demonstration of the JAXA L2 cloud particle category product using actual satellite data could show different preference for the occurrence of different ice habit

https://doi.org/10.5194/amt-2024-99
Preprint. Discussion started: 11 June 2024


Atmospheric Measurement Techniques Discussions

categories. Cloud particle formation and growth conditions can be examined further by incorporating EarthCARE Doppler information.

The active sensor-based JAXA L2 cloud products were assessed using simulated EarthCARE L1 orbit data created by the JAXA joint simulator, covering representative cloud and precipitation scenes over the globe. A comparison of retrieved and modelled microphysics obtained using the AC_CLP standard outputs as a reference showed that the retrieval reasonably reproduced the vertical profile of the modeled microphysics and the majority of the retrieved population of particle size and water content lay close to the 1:1 line with the slopes of the regression lines to be around 0.8 for both the ice and liquid phases. Velocity-related products from the JAXA L2 research cloud product and further improvements in the microphysics retrieval from the CPR–ATLID–MSI synergy will be reported in a future study.

In addition to assessing the L2 cloud product using simulated EarthCARE L1 data, ongoing studies will characterize the product in the framework of JAXA EarthCARE CAL/VAL activity. These studies include the use of ground-based radar and synergistic sensors at the NICT intensive observation site (Okamoto et al., 2024), complementary data from other spaceborne sensors such as A-TRAIN (Sato and Okamoto, 2023), and a European Union–Japanese collaboration to evaluate CPR Doppler measurements and precipitation in CPR blind zones over Antarctica. As part of this joint activity, a validation methodology for space-borne Doppler radar was developed to obtain an unattenuated 94-GHz Doppler spectrum and related information on particle shape, sedimentation velocity, and size distribution at high temporal resolution from disdrometer and 24-GHz (K-band) Doppler radar synergy through frequency conversion and appropriate sampling strategies (Bracci et al., 2023). These validation datasets are highly valuable and will be used for further evaluation of the algorithms for EarthCARE, launched on 28 May.

https://doi.org/10.5194/amt-2024-99
Preprint. Discussion started: 11 June 2024

Atmospheric Measurement Techniques Discussions

Data availability.

The JAXA L2 Echo products, ATLID products, and MSI products were processed by the National Institute of Information and Communications Technology (PI: Horie H.), National Institute for Environmental Studies (PI: Nishizawa, T.) and Tokai University (PI: Nakajima, Y. T.), respectively. The JAXA EarthCARE synthetic data is distributed from https://doi.org/10.5281/zenodo.7835229 (Roh et al., 2023). The CALIPSO Lidar Level 1B profile data V4-10 and CloudSat 2B-GEOPROF P1_R05 data used in this study are provided from the NASA Langley Research Center Atmospheric Science Data Center (https://doi.org/10.5067/CALIOP/CALIPSO/LID_L1-STANDARD-V4-10, NASA/LARC/SD/ASDC, 2016) and CloudSat Data Processing Center (https://www.cloudsat.cira.colostate.edu/data-products/2b-geoprof, Marchand & Mace, 2018), respectively. The KU CloudSat-CALIPSO Merged Data set is provided and updated to the latest version by JAXA A-Train Product Monitor (http://www.eorc.jaxa.jp/EARTHCARE/research_product/ecare_monitor_e.html).

Author contributions.

KS conducted research and drafted the paper. KS and HO developed the active-sensor based JAXA L2 cloud algorithms. TN, YJ, RK, and TYN, MW processed the L1 data and produced the ATLID and MSI L2 products, respectively. MS and RW developed the EarthCARE synthetic data and provided the model outputs. HI provided scattering simulations. All provided useful discussions for the assessment of L2 cloud products.

Competing interests.

The authors have no competing interests to declare.

Special issue statement.

This article is part of the special issue “EarthCARE Level 2 algorithms and data products.” It is not associated with a conference.

Acknowledgements.

The authors would like to thank the JAXA EarthCARE Science Team and the Remote Sensing Technology Center of Japan (RESTEC).

Financial support.

This study was supported by The Japan Aerospace Exploration Agency for the EarthCARE mission (grant no. 24RT000193; 24RT000246); JSPS (KAKENHI Grants JP22K03721; JP24H00275); Research Institute for Applied Mechanics, Kyushu University (Fukuoka, Japan).

https://doi.org/10.5194/amt-2024-99
Preprint. Discussion started: 11 June 2024

Atmospheric Measurement Techniques Discussions

References

Borovoi, A., Konoshonkin, A., Kustova, N., & Okamoto, H. (2012). Backscattering Mueller matrix for quasi-horizontally oriented ice plates of cirrus clouds: Application to CALIPSO signals. *Optics Express*, *20*(27), 28222–28233. https://doi.org/10.1364/oe.20.028222

Bracci, A., Sato, K., Baldini, L., Porcù, F., and Okamoto, H.: Development of a methodology for evaluating spaceborne W-band Doppler radar by combined use of Micro Rain Radar and a disdrometer in Antarctica, Remote Sensing of Environment, 294, 113630, https://doi.org/10.1016/j.rse.2023.113630, 2023.

Hagihara, Y., Okamoto, H., Yoshida, R., Development of a combined CloudSat-CALIPSO cloud mask to show global cloud distribution. *Journal of Geophysical Research*, 15,1–17. https://doi.org/10.1029/2009JD012344, 2010

Ishimoto, H., Radar Backscattering Computations for Fractal-Shaped Snowflakes, J. Meteorol. Soc. Jpn., 86(3), 459–469, doi:10.2151/jmsj.86.459, 2008.

Ishimoto H., K. Masuda, Y. Mano, N. Orikasa, A. Uchiyama,Irregularly shaped ice aggregates in optical modeling of convectively generated ice clouds,Journal of Quantitative Spectroscopy and Radiative Transfer,Volume 113, Issue 8, https://doi.org/10.1016/j.jqsrt.2012.01.017.2012,

Jin, Y., Nishizawa, T., Sugimoto, N., Ishii, S., Aoki, M., Sato, K., and Okamoto, H.: Development of a 355-nm high-spectral-resolution lidar using a scanning Michelson interferometer for aerosol profile measurement, Opt. Express, 28, 23209, https://doi.org/10.1364/oe.390987, 2020.

Jin, Y., T. Nishizawa, N. Sugimoto, S. Takakura, M. Aoki, S. Ishii, A. Yamazaki, R. Kudo, K. Yumimoto, K. Sato and H. Okamoto, Demonstration of aerosol profile measurement with a dual-wavelength high-spectral-resolution lidar using a scanning interferometer, Appl. Opt. 61, 3523-3532, 2022

Kikuchi, M., Okamoto, H., Sato, K., Suzuki, K., Cesana, G., Hagihara, Y., Takahashi, N., Hayasaka, T., and Oki, R.: Development of Algorithm for Discriminating Hydrometeor Particle Types With a Synergistic Use of CloudSat and CALIPSO, JGR Atmospheres, 122, https://doi.org/10.1002/2017jd027113, 2017

Kudo R., Nishizawa T., Aoyagi T.: Vertical profiles of aerosol optical properties and the solar heating rate estimated by combining sky radiometer and lidar measurements. Atmos. Meas. Tech., 9, 3223-3243, 2016.

Kudo, R., Higurashi, A., Oikawa, E., Fujikawa, M., Ishimoto, H., and Nishizawa, T.: Global 3-D distribution of aerosol composition by synergistic use of CALIOP and MODIS observations, Atmos. Meas. Tech., 16, 3835–3863, https://doi.org/10.5194/amt-16-3835-2023, 2023.

Letu, H., Ishimoto, H., Riedi, J., Nakajima, T. Y., C.-Labonnote, L., Baran, A. J., et al. Investigation of ice particle habits to be used for ice cloud remote sensing for the GCOM-C satellite mission. *Atmospheric Chemistry and Physics*, *16*(18), 12287–12303. https://doi.org/10.5194/ acp-16-12287-2016, 2016

Li, M., Letu, H., Peng, Y., Ishimoto, H., Lin, Y., Nakajima, T. Y., et al. Investigation of ice cloud modeling capabilities for the irregularly shaped Voronoi ice scattering models in climate simulations. *Atmospheric Chemistry and Physics*, *22*(7), 4809–4825. https://doi.org/10.5194/ acp-22-4809-2022, 2022

Marchand, R., & Mace, G., Level 2 GEOPROF Product Process Description and Interface Control Document. Retrieved from https://www.cloudsat.cira.colostate.edu/cloudsat-static/info/dl/2b-geoprof/2B-GEOPROF_PDICD.P1_R05.rev0__0.pdf, 2018

Masuda, K., Ishimoto, H., & Mano, Y. Efficient method of computing a geometric optics integral for light scattering by nonspherical particles. Papers in Meteorology and Geophysics, 63, 15–19. https://doi.org/10.2467/mripapers.63.15, 2012

Nakajima, T.Y., Ishida, H., Nagao, T.M., Hori, M., Letu, H., Higuchi, R., Tamaru, N., Imoto, N., Yamazaki, A., Theoretical basis of the algorithms and early phase results of the GCOM-C (Shikisai) SGLI cloud products. https://doi.org/10.1186/s40645-019-0295-9, 2019

Nishizawa, T., Kudo, R., Oikawa E., Higurashi A., Jin, Y., Takakura S., Sugimoto, N., Fujikawa, M., Sato, K., and Okamoto, H.,Retrieval of aerosol optical properties from the EarthCARE high-spectral resolution lidar measurements, Atmos. Meas. Tech., submitted, 2024.

Okamoto, H., K. Sato, Y. Hagihara, Global analysis of ice microphysics from CloudSat and CALIPSO: incorporation of specular reflection in lidar signals, J. Geophys. Res., 115, D22209, doi:10.1029/2009JD013383, 2010.

Okamoto, H., Sato, K., Borovoi, A., Ishimoto, H., Masuda, K., Konoshonkin, A., and Kustova, N.: Interpretation of lidar ratio and depolarization ratio of ice clouds using spaceborne high-spectral-resolution polarization lidar, Opt. Express, 27, 36587, https://doi.org/10.1364/oe.27.036587, 2019.

Okamoto, H., Sato, K., Borovoi, A., Ishimoto, H., Masuda, K., Konoshonkin, A., and Kustova, N.: Wavelength dependence of ice cloud backscatter properties for space-borne polarization lidar applications, Opt. Express, 28, 29178, https://doi.org/10.1364/oe.400510, 2020.

Okamoto, H., Sato, K., Oikawa, E., Ishimoto, H., Ohno, Y., Horie, H., Hagihara, Y., Nishizawa, T., Kudo, R., Higurashi, A., Jin, Y., Nakajima, T. Y., Wang, M., Roh, W., Satoh, M., Suzuki,K., Kubota, T.Tanaka, T.,Yamauchi,A.,Sekiguchi,M.,and Nagao,T.M., Overview of EarthCARE JAXA Level 2 algorithms, Atmos. Meas. Tech., submitted , 2024

Okamoto, H., Sato, K., Oikawa, E., Hagihara, Y., Shaik, A., Nishizawa, T., Cloud mask and particle type classification using EarthCARE CPR and ATLID, Atmos. Meas. Tech., in preparation, 2024b.

Roh, W., Satoh, M., Hashino, T., Matsugishi, S., Nasuno, T., and Kubota, T.: Introduction to EarthCARE synthetic data using a global storm-resolving simulation, Atmos. Meas. Tech., 16, 3331–3344, https://doi.org/10.5194/amt-16-3331-2023, 2023.

Satoh, M., Tomita, H., Yashiro, H., Miura, H., Kodama, C., Seiki, T., Noda, A. T., Yamada, Y., Goto, D., Sawada, M., Miyoshi, T., Niwa, Y., Hara, M., Ohno, T., Iga, S., Arakawa, T., Inoue, T., and Kubokawa, H.: The Non-hydrostatic Icosahedral Atmospheric Model: description and development, Progress in Earth and Plan- etary Science, 1, 18, https://doi.org/10.1186/s40645-014-0018-1, 2014.

Sato, K., Okamoto, M. K. Yamamoto. S. Fukao, H. Kumagai, Y. Ohno, H. Horie,and M. Abo 95-GHz Doppler radar and lidar synergy for simultaneous ice microphysics and in-cloud vertical air motion retrieval. J. Geophys. Res., 114, D03203, doi:10.1029/2008JD010222, 2009.

Sato, K. and H. Okamoto, Refinement of global ice microphysics using spaceborne active sensors, J. Geophys. Res.,116, D20202, doi:10.1029/2011JD015885, 2011

Sato, K., H. Okamoto, H. Ishimoto, Physical model for multiple scattered space-borne lidar returns from clouds, Opt. Express 26, A301-A319, doi.org/10.1364/O E.26.00A301, 2018.

Sato, K., H. Okamoto, H. Ishimoto, Modeling the depolarization of space-borne lidar signals. Opt. Express, 27, A117-A132, doi:10.1364/OE.27.00A117, 2019

Sato, K., Okamoto, H., Application of single and multiple-scattering theories to analysis of space-borne cloud radar and lidar data, Springer Nature, Springer Series in Light Scattering, Vol.5, pp.1-37, doi:10.1007/978-2-030-38696-2 , 2020

Sato, K. and Okamoto, H.: Global Analysis of Height-Resolved Ice Particle Categories From Spaceborne Lidar, Geophysical Research Letters, 50, https://doi.org/10.1029/2023gl105522, 2023.

Sullivan S., D. Lee, L.Oreopoulos, A. Nenes, Role of updraft velocity in temporal variability of global cloud hydrometeor number, PNAS, https://www.pnas.org/doi/10.1073/pnas.1514039113, 2016

Van Diedenhoven, B. (2018). Remote sensing of crystal shapes in ice clouds. In A. Kokhanovsky (Ed.), *Springer series in light scattering*, *Springer series in light scattering*. Springer. https://doi.org/10.1007/978-3-319-70808-9_5

Wang, M., Nakajima, TY., Roh, W., Satoh, M., Suzuki, K., Kubota, T., Yoshida, M., Evaluation of the spectral misalignment on the Earth Clouds, Aerosols and Radiation Explorer/multi-spectral imager cloud product, Atmos. Meas. Tech., 16, 603-623, https://doi.org/10.5194/amt-16-603-2023,2023

Yamauchi, A., Suzuki, K., Oikawa, E., Sekiguchi, M., Nagao, T. M, and Ishida, H.: Description and validation of the Japanese algorithm for radiative flux and heating rate products with all four EarthCARE instruments : Pre-launch test with A-Train, Atmos. Meas. Tech. Discuss., 2024.

Yoshida, R., Okamoto, H., Hagihara, Y., and Ishimoto, H.: Global analysis of cloud phase and ice crystal orientation from Cloud-Aerosol Lidar and Infrared Pathfinder Satellite Observation (CALIPSO) data using attenuated backscattering and depolarization ratio, J. Geophys. Res., 115, https://doi.org/10.1029/2009jd012334, 2010.